Current Optics and Photonics
Vol. 2, No. 2, April 2018, pp. 134-139

ISSN: 2508-7266(Print) / ISSN: 2508-7274(Online)
DOI: https://doi.org/10.3807/COPP.2018.2.2.134

Photonic Generation of Frequency-tripling Vector Signal Based on Balanced Detection without Precoding or Optical Filter

Kun Qu[1]*, Shanghong Zhao[1], Xuan Li[1], Zihang Zhu[1], and Qinggui Tan[2]

[1]Air Force Engineering University, Xi'an 710000, China
[2]China Academy of Space Technology, Xi'an 710000, China

(Received September 14, 2017 : revised January 4, 2018 : accepted January 31, 2018)

A novel approach for frequency-tripling vector signal generation via balanced detection without precoding and optical filter is proposed. The scheme is mainly utilizing an integrated dual-polarization quadrature phase shift keying (DPQPSK) modulator. In the DPQPSK modulator, one QPSK modulator is driven by an RF signal to generate high-order optical sidebands, while the other QPSK modulator is modulated by I/Q data streams to produce baseband vector signal as an optical carrier. After that, a frequency-tripling 16-quadrature-amplitude-modulation (16QAM) vector millimeter-wave (mm-wave) signal can be obtained by balanced detection. The proposed scheme can reduce the complexity of transmitter digital signal processing. The results show that, a 4 Gbaud baseband 16QAM vector signal can be generated at 30 GHz by frequency-tripling. After 10 km single-mode fiber (SMF) transmission, the constellation and eye diagrams of the generated vector signal perform well and a bit-error-rate (BER) below than 1e-3 can be achieved.

Keywords : Vector signal generation, Frequency-tripling, Balanced detection
OCIS codes : (060.2330) Fiber optics communications; (060.4080) Modulation; (060.4510) Optical communications

I. INTRODUCTION

With the increasing demand for huge bandwidth and long-distance ultra-capacity services of communication network, mm-wave communication system based on the radio-over-fiber and integrated optics has been perceived as a promising candidate for the future wireless communication and space communication [1-3]. Conventionally, mm-wave signal is always generated in the electrical domain but suffers from low carrier frequency and the insufficient bandwidth of electrical components [4-8]. To overcome these problems, mm-wave signals generation based on photonics technologies have been widely investigated, which is of great significance for breaking electronic bandwidth bottleneck, thanks to the inherent advantages such as high frequency, wide bandwidth, large tunability and immunity to electromagnetic interference. Additionally, vector modulated mm-wave signal can efficiently overcome the limitation of insufficient spectrum resources and provide higher data transmission. Thus, various approaches have been proposed to generate vector mm-wave signals based on photonic technology.

Recently, several feasible schemes for vector mm-wave signal generation based on precoding assisted photonic frequency multiplication technique have been investigated [9-11]. One scheme for generation of QPSK vector signal based on frequency octupling and precoding is proposed in [9], the generation of QPSK and 16 QAM vector signal also utilized precoding technique based on frequency quadrupling and frequency doubling is proposed in [10] and [11], respectively. These schemes can generate high frequency vector mm-wave signal with the reduction of the bandwidth requirement for both optical and electrical components, but they all need an additional, expensive wavelength filter to select the two optical subcarriers, which will decrease the signal-to-noise (SNR). As an improvement, some other schemes for vector mm-wave signal generation based on

*Corresponding author: m13259463680@163.com, ORCID 0000-0003-4361-7425
Color versions of one or more of the figures in this paper are available online.

precoding that without wavelength filter are proposed [12, 13], one scheme for vector signal generation by only one single-drive MZM without optical filter is proposed in [12], it can realize frequency-quadrupling QPSK vector signal generation, but the optical suppression ratio between the sideband of second order and the fourth order is only 10 dB, which will decrease the SNR and is not suitable for high order QAM vector signal generation. Another scheme can generate high order vector signal based on precoding without optical filter, but it only can generate frequency-doubling vector signal [13]. However, the schemes that mentioned above all utilized precoding technique, which are needed to address the phase multiplication induced by the frequency multiplication, which will increase the complexity of transmitter digital signal processing (DSP) [14]. So [14] proposed a scheme for vector signal generation enabled by a single-drive MZM without precoding and optical filter, but it also needs the transmitter DSP to get the driven signal and only gets a frequency-doubling vector signal.

In this paper, we propose an all-optical frequency-tripling vector signal generator based on an integrated DPQPSK modulator and balanced detection. In our proposed scheme, an rf signal is applied to the upper QPSK modulator and configured to generate a frequency-sextupling signal, while the bottom QPSK modulator is driven by the I/Q data streams and configured to generate a baseband vector signal carried by the optical carrier. Then the two optical signals are combined through the polarization beam combiner (PBC) and sent to a balanced photodetector (BPD). Finally a frequency-tripling vector signal can be obtained. Employing our proposed scheme, we demonstrate a 10 GHz, 4 Gbaud 16QAM mm-wave vector signal generated at 30 GHz by frequency-tripling. The results show that, the 30 GHz 4 Gbaud vector signal can achieve a BER below than 1e-3 after 10 km SMF transmission. The constellation and the eye diagrams have a good performance. Compared with the previous reports, our scheme has a simple structure as the use of only one modulator without precoding or optical filter. Meanwhile, this scheme can satisfy the requirement of high frequency application and high order vector modulation because of frequency-tripling and 16QAM modulation. Furthermore, the generated vector signal can immune to background noise and higher order distortion due to the balanced detection.

II. PRINCIPLE

Figure 1(a) demonstrates the frame of the frequency-tripling 16QAM vector signal generator. It mainly contains a laser diode (LD), a DPQPSK modulator, a polarization beam splitter (PBS) and a BPD. The DPQPSK modulator integrates a Y-splitter, two QPSK modulators, a 3-dB optical couple and a PBC. There are two sub-MZMs embedded in a main MZM for each of the QPSK modulators. As depicted in Fig. 1, a lightwave from the LD is launched to the DPQPSK modulator via PC1. Then the lightwave is power halved by the Y-splitter and injected into two paths, which are modulated by two electrical driving signals in the two QPSK modulators respectively, a PBC is used to combine the two signals with orthogonal polarization states. Figure 1(b) shows the schematic diagram of the optical sidebands and their polarization states, it can be seen that the two signals have orthogonal polarization states at the output of DPQPSK modulator by adjusting the PBC.

In the DPQPSK modulator, the upper QPSK modulator is modulated by an RF signal from a microwave signal generator (MSG), in where sub-MZM1 and sub-MZM2 are driven by the RF signal with the same frequency but 3π/5 phase difference. When both the sub-MZMs are biased at the minimum transmission point and the main MZM biased at the maximum transmission point, the optical signal at the output of the upper QPSK modulator can be expressed as

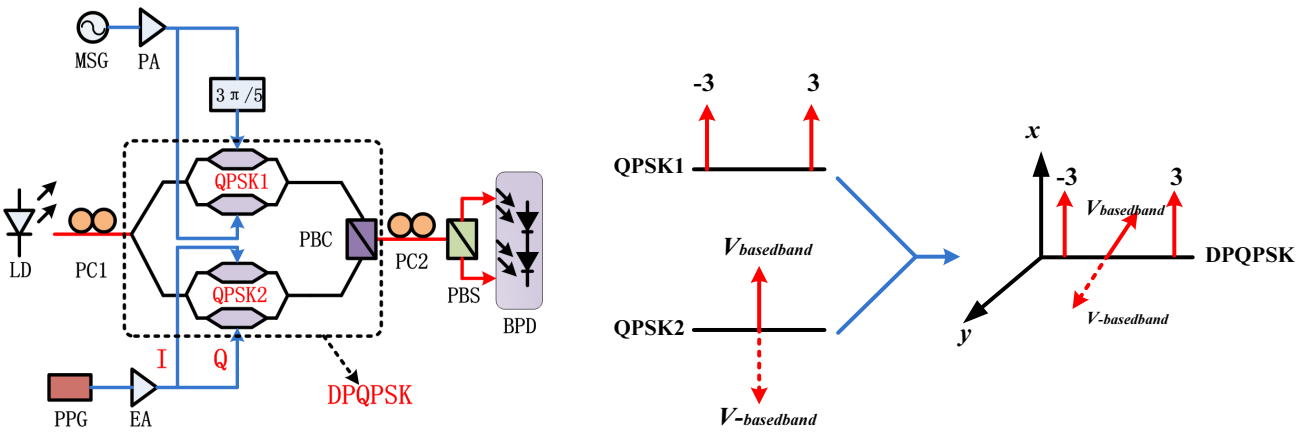

FIG. 1. (a) Schematic diagram for the generation of 16QAM vector signal (b) Schematic diagram of the optical sidebands from the outputs of the modulators.

$$E_a = \frac{\sqrt{2}}{8} E_c e^{j\omega_c t + j\frac{\pi}{2}} \left\{ e^{jm\cos(\omega_m t)} - e^{-jm\cos(\omega_m t)} + e^{jm\cos(\omega_m t + \phi)} - e^{-jm\cos(\omega_m t + \phi)} \right\}$$
$$= \frac{\sqrt{2}}{8} E_c e^{j\omega_c t} \sum j^n J_n(m) \sin\left(\frac{n\pi}{2}\right) [1 + e^{jn\phi}] e^{jn(\omega t + \frac{\pi}{2})}$$
$$= \frac{\sqrt{2}}{2} E_c e^{j\omega_c t} \sum_{n=-\infty}^{\infty} J_3(m) e^{j(\omega_c + 3\omega_m)t} \quad (1)$$

where E_c and ω_c are the amplitude and angular frequency of the optical carrier, respectively. ω_m is the angular frequency of the RF signal. $m = \frac{\pi v_m}{2v_\pi}$ is modulation index of the upper QPSK modulator, where v_π and v_m denote the half-wave voltage and driving voltage, respectively. J_n is the nth-order Bessel function of the first kind, ϕ is the phase difference between the sub-MZMs.

The bottom QPSK modulator in the DPQPSK is used to generate a baseband vector signal and the sub-MZMs of the QPSK modulator are configured as inphase and quadrature branches modulated by two binary data sequences I(t) and Q(t). The output optical signal of this QPSK modulator can be written as

$$E_b = \frac{\sqrt{2}}{4} E_c e^{j\omega_c t} [I(t) + jQ(t)] \quad (2)$$

The optical signals from the two QPSK modulators are combined by the PBC with orthogonal polarization states. Then the signal is split by the PBS via another PC2. By adjusting PC2 to an angle of 45° with respect to one principle axis of the PBS, the two optical signals from two output ports of the PBS can be respectively expressed as

$$E_{1,2} = \frac{\sqrt{2}}{4} [2\vec{x} E_a \pm \vec{y} E_b] \quad (3)$$

where x and y are the polarization states of the two orthogonal signals, respectively.

Then the optical signals from PBS are converted to electrical signal by the BPD and the signal at the BPD can be respectively expressed as

$$I_1 = R[E_1 E_1^*] = \frac{R}{8} E_c^2 \left\{ 2J_3^2(m)\cos 3\omega_m t + \frac{1}{4}[I(t) + jQ(t)]^2 + 2J_3(m)\cos 3\omega_m t [I(t) + jQ(t)] \right\} \quad (4)$$

$$I_2 = R[E_2 E_2^*] = \frac{R}{8} E_c^2 \left\{ 2J_3^2(m)\cos 3\omega_m t + \frac{1}{4}[I(t) + jQ(t)]^2 - 2J_3(m)\cos 3\omega_m t [I(t) + jQ(t)] \right\} \quad (5)$$

R is the response of the BPD and * represents a complex conjugate. The final electrical signal from the BPD can be expressed as

$$I_1 - I_2 = \frac{R}{4} E_c^2 2J_3(m)\cos 3\omega_m t [I(t) + jQ(t)] \quad (6)$$

As can be seen from Eq. (6), a vector signal at the frequency of $3\omega_m$ can be generated.

III. SIMULATION RESULTS AND DISCUSSION

To investigate the performance of the proposed frequency-tripling vector signal generator, a simulation is conducted by using Optisystem, and the results are then compared with the mathematical analysis. In the simulation, the lightwave has a frequency of 193.1 THz and a power of

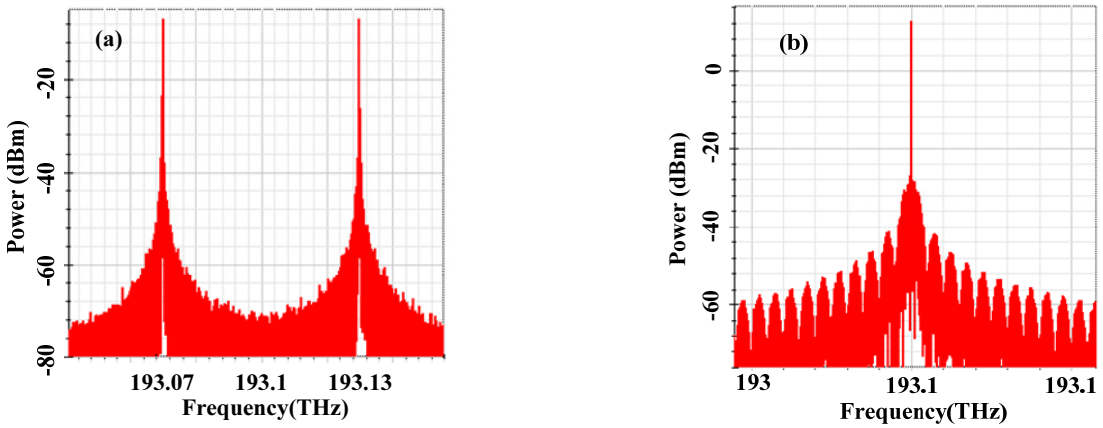

FIG. 2. Optical spectra at the output of two QPSK modulators in the DP-QPSK modulator (a) the upper QPSK modulator is configured to generate a frequency-sextupling signal, (b) the bottom QPSK modulator is configured to generate a baseband vector signal.

10 dBm with 100 kHz linewidth, the half-wave voltage for the MZMs is 3V. The upper QPSK modulator is driven by an RF signal at 10 GHz and modulation index m is set as 3.83 to make $J_1(m)=0$. The phase difference ϕ of the two sub-MZMs in the upper QPSK modulator is set as 3π/5 to make $J_5(m)=0$. The bottom QPSK modulator is driven by a 16QAM vector signal at 4 Gbaud, which is generated from the pulse pattern generator (PPG) with a pseudorandom binary sequence (PRBS) of $2^{13}-1$.

The optical spectra obtained from the upper and bottom QPSK modulators are shown in Figs. 2(a) and 2(b), respectively. As can be seen from Fig. 2(a), the ±3st-order sidebands are clearly generated. Figure 2(b) shows the optical spectra of the baseband vector signal carried by the original optical carrier.

After tuning PC2 to make the polarization state of E_a or E_b has an angle of 45° to one principle axis of the PBS, the optical spectra from the two ports of the PBS can be measured in Figs. 3(a) and 3(b), respectively. It can be seen that the optical carrier consists of the baseband vector information and ±3st-order sidebands are obtained in the two ports.

Then a frequency-tripling vector signal can be generated when the two optical signal from the two ports of PBS are detected by BPD. To eliminate the electrical spurious components caused by the seven-order optical spurious sideband, a bandpass filter is placed after the BPD. Figure 4(a) shows the electrical spectra of the generated vector signal, it can be found that a peak located at 30 GHz, which is consistent with our derivation in Eq. (6). The corresponding constellations for the 4 Gbaud 16QAM vector signal at 30 GHz are illustrated in Fig. 4(b), which validate its feasibility to generate high frequency mm-wave vector signal.

In order to evaluate the quality of the generated 16QAM vector signal, the BER of the signal as a function of the input optical power for back-to-back (BTB) and 10 km SMF transmission are measured, and it is measured by comparing the data recovered from the received signal with the original transmitter data. Figure 5(a) shows the measured BER curves of the 4 Gbaud 16QAM vector signal at 30 GHz in the condition of BTB and 10 km SMF transmission, it can be seen the BER of less than 1e-3 can be achieved when the power of optical signal

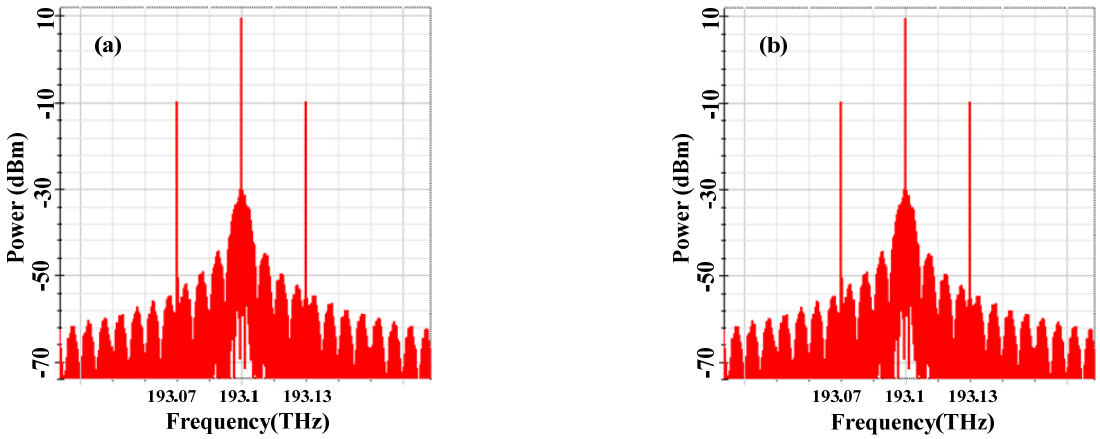

FIG. 3. Optical spectra of the signals split by the PBS.

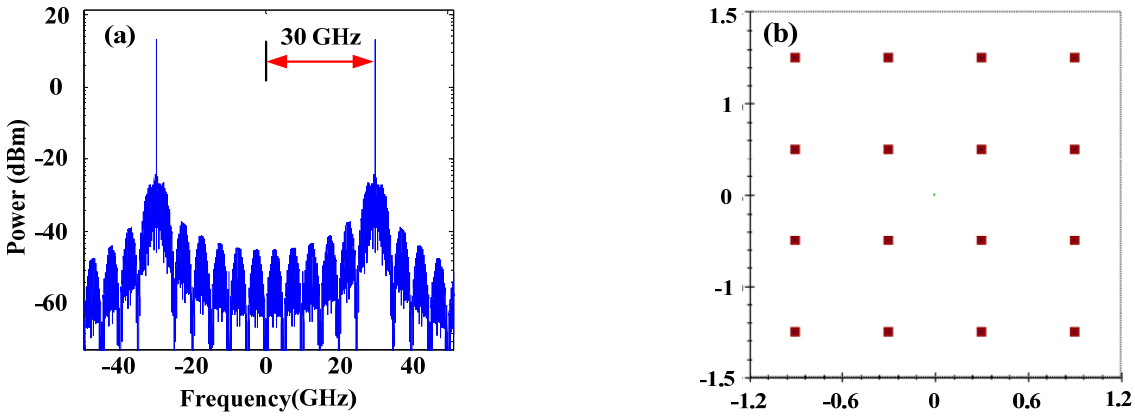

FIG. 4. (a) The electrical spectra of the generated 16QAM vector signal at 30 GHz (b) The constellation of the generated 16QAM vector signal.

received by the BPD is beyond about 0.5 dBm and 2.7 dBm in the condition of BTB and 10 km SMF transmission, respectively. Compared with the BTB transmission, the performance of the 10 km SMF transmission will be affected by the fiber transmission loss, which will reduce the optical signal-to-noise ratio (OSNR), so it can be seen that 10 km SMF transmission causes a 2.2 dB power penalty. When the input power is increased, the OSNR will also be increased, which will reduce the BER of the transmission signals. Additionally, the corresponding received 16QAM constellation with BPD input power at 4 dBm is shown in Fig. 5(b), it can be seen that the constellation is clear and almost symmetrical. These results demonstrate the feasibility and validate the superiority of this proposal.

Meanwhile, Figs. 6(a) and 6(b) show the eye diagrams of the I and Q branches when the generated 16QAM mm-wave signal is demodulated by a 30 GHz local oscillator signal after 10 km SMF transmission. As can be seen, the eyes are opening well.

IV. CONCLUSION

In conclusion, we have proposed a novel photonic frequency-tripling 16QAM vector signal generation scheme based on balanced detection. The key component is a DPQPSK modulator where one QPSK modulator in the DPQPSK is configured to generate a frequency-sextupling optical signal while the other QPSK modulator is configured to generate a baseband vector signal. After combining the two signals by a PBS and through balanced detection, a frequency-tripling vector signal can be generated. Because only one modulator is used and there is no precoding technique and optical filter existed, the system has simple structure and there is no need for transmitter DSP. Furthermore, we demonstrate that the generated 4 Gbaud 30 GHz 16QAM vector signal can be transmitted over 10 km SMF, with the simulated BER results under 1e-3, and the eye diagrams and constellation have a good performance.

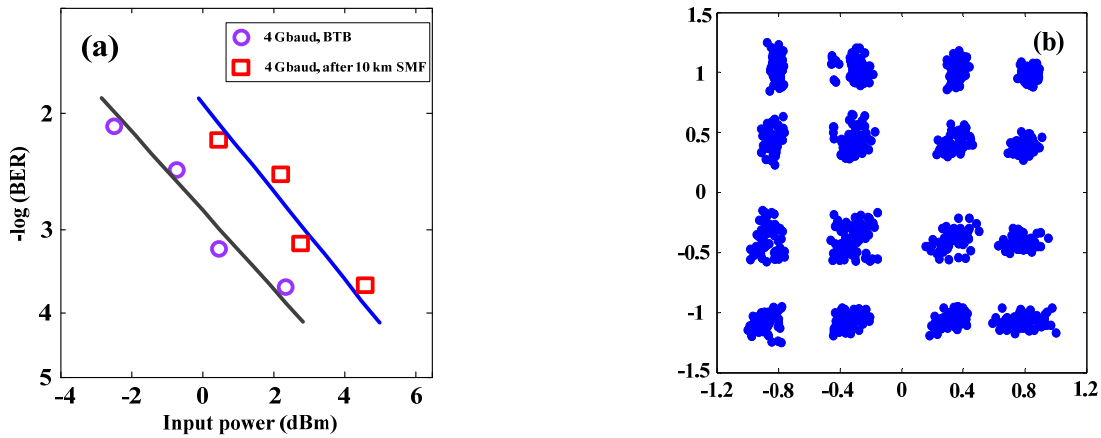

FIG. 5. (a) BER versus BPD input power in the case of BTB and 10 km SMF transmission (b) The corresponding constellation of 16QAM vector signal in 10 km SMF transmission case with BPD input power at 4 dBm.

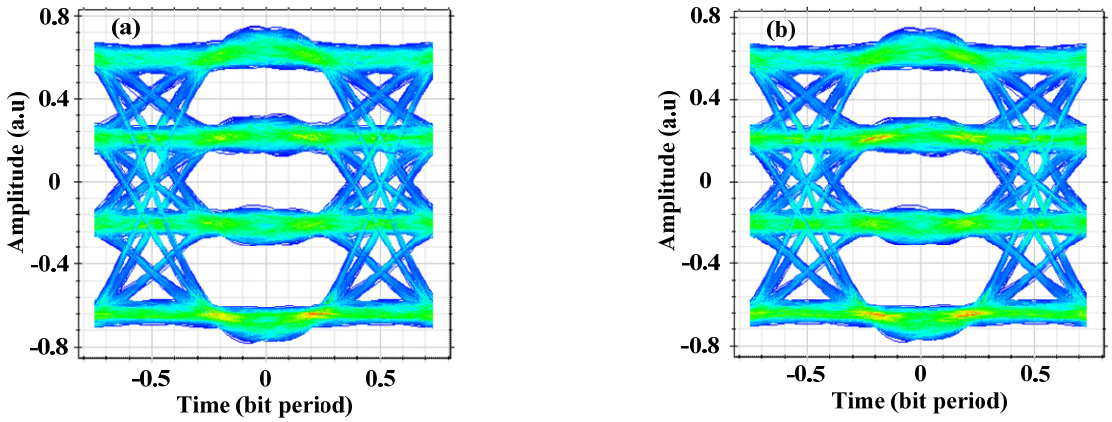

FIG. 6 The eye diagrams of (a) I branch and (b) Q branch of the generated 16QAM signal at 30 GHz after 10 km SMF transmission.

ACKNOWLEDGEMENT

This work was supported in part by the National Natural Science Foundation of China (No. 61231012) and Natural Science Foundation of Shaan'xi Province (No. 2016JM6073).

REFERENCES

1. K. Kitayama, A. Maruta, and Y. Yoshida, "Digital coherent technology for optical fiber and radio-over-fiber transmission systems," J. Lightw. Technol. **32**, 3411-3420 (2014).
2. H. T. Huang, W. L. Liang, C. T. Lin, C. C. Wei, and S. Chi, "100-GHz DD-OFDM-RoF system over 150-km fiber transmission employing pilot-aided phase noise suppression and bit-loading algorithm," Opt. Express **22**, 3938-3943 (2014).
3. X. Li, Z. Dong, J. Yu, N. Chi, Y. Shao, and G. K. Chang, "Fiber-wireless transmission system of 108 Gb/s data over 80 km fiber and 2 × 2 multiple-input multiple-output wireless links at 100 GHz W-band frequency," Opt. Lett. **37**, 5106-5108 (2012).
4. J. Yu, Z. Jia, L. Yi, Y. Su, G.-K. Chang, and T. Wang, "Optical millimeter-wave generation or up-conversion using external modulators," IEEE Photon. Technol. Lett. **18**, 265-267 (2006).
5. C.-T. Lin, P.-T. Shih, W.-J. Jiang, E.-Z. Wong, J. J. Chen, and S. Chi, "Photonic vector signal generation at microwave/millimeter-wave bands employing an optical frequency quadrupling scheme," Opt. Lett. **34**, 2171-2173 (2009).
6. W. Li and J. Yao, "Microwave generation based on optical domain microwave frequency octupling," IEEE Photon. Technol. Lett. **22**, 24-26 (2010).
7. J. Zhang, H. Chen, M. Chen, T. Wang, and S. Xie, "A photonic microwave frequency quadrupler using two cascaded intensity modulators with repetitious optical carrier suppression," IEEE Photon. Technol. Lett. **19**, 1057-1059 (2007).
8. J. Yu, Z. Jia, T. Wang, and G. K. Chang, "Centralized lightwave radio-over-fiber system with photonic frequency quadrupling for high-frequency millimeter-wave generation," IEEE Photon. Technol. Lett. **19**, 1499-1501 (2007).
9. X. Li, J. Yu, J. Xiao, N. Chi, and Y. Xu, "W-band PDM-QPSK vector signal generation by MZM-based photonic frequency octupling and precoding," IEEE Photon. J. **7**, 7101906 (2015).
10. X. Li, J. Zhang, J. Xiao, Z. Zhang, Y. Xu, and J. Yu, "W-band 8QAM vector signal generation by MZM-based photonic frequency octupling," IEEE Photon. Technol. Lett. **27**, 1257-1260 (2015).
11. L. Zhao, J. Yu, L. Chen, P. Min, J. Li, and R. Wang, "16QAM vector millimeter-wave signal generation based on phase modulator with photonic frequency doubling and precoding," IEEE Photon. J. **8**, 5500708 (2016).
12. X. Li, J. Yu, and G. Chang, "Frequency-quadrupling vector mm-wave signal generation by only one single-drive MZM," IEEE Photon. Technol. Lett. **28**, 1302-1305 (2016).
13. Z. Dong, "64QAM vector radio-frequency signal generation based on phase precoding and optical carrier suppression modulation" IEEE Photon. J. **8**, 2630306 (2016).
14. Y. Wang, J. Yu, X. Li, Y. Xu, N. Chi, G.-K. Chang, "Photonic vector signal generation employing a single-drive MZM-based optical carrier suppression without precoding" J. Lightw. Technol. **33**, 5235-3241 (2015).